Development 128, 4899-4910 (2001)
Printed in Great Britain © The Company of Biologists Limited 2001
DEV2723



# Overlapping functions of lysosomal acid phosphatase (LAP) and tartrate-resistant acid phosphatase (Acp5) revealed by doubly deficient mice

**Anke Suter[1], Vincent Everts[2], Alan Boyde[3], Sheila J. Jones[3], Renate Lüllmann-Rauch[4], Dieter Hartmann[4], Alison R. Hayman[5], Timothy M. Cox[5], Martin J. Evans[5], Tobias Meister[1], Kurt von Figura[1] and Paul Saftig[1,*]**

[1]Zentrum Biochemie und Molekulare Zellbiologie, Abt. Biochemie II, Universität Göttingen, Heinrich-Düker-Weg 12, 37073 Göttingen, Germany
[2]Department of Cell Biology, AMC, Meibergdreef 15, 1105 AZ Amsterdam, and Department of Periodontology, ACTA, University of Amsterdam The Netherlands
[3]Department of Anatomy and Developmental Biology, University College London, Gower Street, London WC1E 6BT, UK
[4]Anatomisches Institut, Christian Albrechts Universität Kiel, 24118 Kiel, Germany
[5]Department of Medicine, University of Cambridge, Level 5, Addenbrooke's Hospital, Cambridge CB2 2QQ, UK; Wellcome Trust, Institute of Cancer and Developmental Biology; and Department of Genetics, University of Cambridge CB2 1QR, UK
*Author for correspondence (e-mail: psaftig@gwdg.de)

*Accepted 31 August 2001*

## SUMMARY

**To date, two lysosomal acid phosphatases are known to be expressed in cells of the monocyte/phagocyte lineage: the ubiquitously expressed lysosomal acid phosphatase (LAP) and the tartrate-resistant acid phosphatase-type 5 (Acp5). Deficiency of either acid phosphatase results in relatively mild phenotypes, suggesting that these enzymes may be capable of mutual complementation. This prompted us to generate LAP/Acp5 doubly deficient mice. LAP/Acp5 doubly deficient mice are viable and fertile but display marked alterations in soft and mineralised tissues. They are characterised by a progressive hepatosplenomegaly, gait disturbances and exaggerated foreshortening of long bones. Histologically, these animals are distinguished by an excessive lysosomal storage in macrophages of the liver, spleen, bone marrow, kidney and by altered growth plates. Microscopic analyses showed an accumulation of osteopontin adjacent to actively resorbing osteoclasts of Acp5- and LAP/Acp5-deficient mice. In osteoclasts of phosphatase-deficient mice, vacuoles were frequently found which contained fine filamentous material. The vacuoles in Acp5- and LAP/Acp5 doubly-deficient osteoclasts also contained crystallite-like features, as well as osteopontin, suggesting that Acp5 is important for processing of this protein. This is further supported by biochemical analyses that demonstrate strongly reduced dephosphorylation of osteopontin incubated with LAP/Acp5-deficient bone extracts. Fibroblasts derived from LAP/Acp5 deficient embryos were still able to dephosphorylate mannose 6-phosphate residues of endocytosed arylsulfatase A. We conclude that for several substrates LAP and Acp5 can substitute for each other and that these acid phosphatases are essential for processing of non-collagenous proteins, including osteopontin, by osteoclasts.**

Key words: Bone resorption, Kupffer cells, Osteoclasts, Macrophages, Lysosomal storage, Osteopontin, Mouse

## INTRODUCTION

Acid phosphatases (EC 3.1.3.2) are a family of enzymes that can be differentiated according to structural, catalytic and immunological properties, tissue distribution and subcellular location. So far three isoenzymes of extracytoplasmic acidic phosphatases have been identified that belong to the group of orthophosphoric monoesterases with an acidic pH optimum (Drexler and Gignac, 1994). The highly homologous secretory acid phosphatase of the prostate (PAP), which is specifically expressed and secreted in this gland (Vihko et al., 1988) resembles the ubiquitiously expressed lysosomal acid phosphatase (LAP) in its sensitivity to inhibition by L-tartrate (de Araujo et al., 1976). In addition to the tartrate-sensitive LAP, the tartrate-resistant type 5 acid phosphatase (Acp5) has been identified in the lysosomal compartment (Clark et al., 1989) of cells of the mononuclear phagocytic system (Drexler and Gignac, 1994; Hayman et al., 2000).

LAP (Acp2 – Mouse Genome Informatics) was crucial to the initial discovery of lysosomes by de Duve in 1963 and is widely used as a biochemical marker for lysosomes. It is synthesised as a membrane-bound precursor and transported to the plasma membrane (Hille et al., 1992). Before its delivery to the lysosomes, the precursor recycles from the early endosomes to the cell membrane (Braun et al., 1989). In lysosomes, the soluble mature LAP is released by limited proteolysis (Gottschalk et al., 1989). In vitro, LAP cleaves various phosphomonoesters (e.g. adenosine monophosphate, thymolphthaleinphosphate, *p*-nitrophenyl phosphate and glucose 6-phosphate) at an acidic pH 3.5-5.0 (Gieselmann et

al., 1984), but neither its in vivo substrates nor its functional role is known. LAP-deficient mice have recently been generated in an effort to understand the physiological role of this isoenzyme. Lysosomal storage was found in podocytes and tubular epithelial cells of the kidney. Lysosomal storage was detected in subsets of microglia, ependymal cells and astroglia within the central nervous system, concomitant with the development of a progressive astrogliosis and microglial activation. Conspicuous alterations of bone structure became apparent in mice older than 15 months, which resulted in a kyphoscoliotic malformation of the lower thoracic vertebral column (Saftig et al., 1997).

The tartrate-resistant type 5 acid phosphatase Acp (otherwise known as TRAP and like uteroferrin a member of the purple acid phosphatase family) is another orthophosphoric monoesterase, identified in the lysosomal compartment. Acp5 enzyme activity has been detected in the monocyte/phagocyte system, i.e. alveolar macrophages and osteoclasts (Hayman et al., 2000; Bevilacqua et al., 1991), and it is commonly used as an osteoclast-specific marker (Minkin, 1982). Acp5 is a binuclear iron protein of unknown function, but it promotes the hydrolysis of nucleotides, arylphosphates and phosphoproteins, including osteopontin and bone sialoprotein in vitro (Vincent and Averill, 1990; Andersson and Ek-Ryklander, 1995). To explore the physiological action of this protein, Acp5-deficient mice were generated (Hayman et al., 1996). These mice mature normally but exhibit developmental and modelling deformities of the limb bones and axial skeleton suggesting that Acp5 participates in the early stages of endochondral ossification and maintains integrity and turnover of the adult skeleton by contributing to bone matrix resorption (Hayman et al., 1996). In addition, it has recently been shown that these mice have disordered macrophage inflammatory responses and reduced clearance of the microbial pathogen *Staphylococcus aureus* (Bune et al., 2000).

The functional relationship between the lysosomal proteins LAP and Acp5 is unknown. The different phenotypes of LAP- and Acp5-deficient mice clearly indicate that these two lysosomal phosphatases have distinct functions. The rather mild phenotype of LAP-deficient and of Acp5-deficient mice suggests that the phosphatases may in part substitute for each other. To delineate functions that are shared by both phosphatases, LAP/Acp5 doubly deficient mice were generated. We show that these mice display alterations of greater severity than observed in singly deficient mice (bone abnormalities, storage in glial cells) or alterations not seen at all in single deficient mice (massive lysosomal storage in Kupffer cells and macrophages of bone marrow, spleen and kidney). Additionally, we show that both phosphatases are likely to be involved in the dephosphorylation of osteopontin.

## MATERIALS AND METHODS

### Generation of mice with disruption of LAP and Acp5

LAP-deficient mice (Saftig et al., 1997) and tartrate-resistant acid phosphatase (Acp5) deficient mice (Hayman et al., 1996) were mated. Doubly heterozygote mice ($Lap^{+/-}$; $Acp5^{+/-}$) of the following generation were used for further breeding. One hundred and twelve offspring were generated in 14 litters. Three doubly deficient mice ($Lap^{-/-}$; $Acp5^{-/-}$) were obtained and used for further breeding. The resulting mice, which were deficient for one gene and heterozygote for the other gene, were used for breeding in parallel. From these matings, 66 offspring were obtained with 15 mice doubly deficient for $Lap^{-/-}$ and $Acp5^{-/-}$.

Mice were genotyped using established Southern blot protocols for the targeted *Lap* and *Acp5* gene loci (Saftig et al., 1997; Hayman et al., 1996).

### Subcellular fractionation on Percoll gradients

Liver tissue samples were homogenised (20% w/v) in a Dounce homogeniser (20 strokes) and postnuclear supernatants were prepared in 0.25 M sucrose buffered with 3 mM imidazole/HCl, 1 mM EDTA pH 7.4. 0.2 ml of this supernatant was mixed to a final concentration of 30% Percoll solution (10 ml) in 0.25 M sucrose, 3 mM imidazole/HCl, 1 mM EDTA pH 7.4 and centrifuged for 90 minutes at 55,000 ***g*** in a fixed angle rotor Ti 75 (Beckmann Instruments). Density, β-hexosaminidase, succinate dehydrogenase, NADH-cytochrom-c-reductase, 300 kDa mannose 6-phosphate receptor (Pohlmann et al., 1995) and acid phosphatase activity were determined in each of 20 fractions collected.

### Acid phosphatase assays

Aliquots of the Percoll-enriched lysosomal fractions in 0.1% Triton X-100 were incubated with 100 μl of 10 mM *p*-nitrophenylphosphate in 0.1 M sodium citrate, pH 4.5, and either 50 μl 40 mM NaCl or 50 μl 40 mM tartrate. After incubation, the reaction was stopped by addition of 0.5 ml of 0.4 M glycine/NaOH, pH 10.4. Absorbance at 405 nm was determined. The tartrate-inhibitable LAP activity was determined as described (Waheed et al., 1985). After immunoprecipitation of enriched lysosomal fractions with an anti-uteroferrin antibody (Echetebu et al., 1987), tartrate-resistant acid phosphatase (Acp5) activity of the dissolved immunoprecipitate was determined.

### Endocytosis of [$^{35}$S] or [$^{32}$P] arylsulfatase A

Fibroblasts which are deficient for both mannose 6-phosphate receptors (Kasper et al., 1996) that were transfected with human arylsulfatase-A (ASA) were grown to confluency on 10 cm dishes and labelled overnight with 5.5 MBq [$^{35}$S]methionine or 1.1 MBq [$^{32}$P]orthophosphate. Purification using a column to which an ASA-specific antibody had been coupled and endocytosis of labelled ASA in the presence and absence of 5 mM mannose 6-phosphate has been described previously (Sandholzer et al., 2000).

### Radiographs and bone preparations

Mice were anaesthetised and subjected to radiography (high resolution, soft X-ray system, DIMA Soft P41, Feinfocus, Garbsen, Germany). For each mouse the same radiation energy (30 kV) and exposure times were used. Radiographs were stored as digital files and processed using the FCR 9000 HQ system (Fuji, Düsseldorf, Germany).

Long bones (femora, tibiae, humeri) were dissected free of soft tissues and bone length was measured with fine callipers.

### Histological examinations of soft tissues

For electron microscopy the animals were perfused with 6% glutaraldehyde in 0.1 M phosphate buffer. Tissue samples were post-fixed with 2% osmium tetroxide, dehydrated and embedded in Araldite. Semi-thin sections were stained with Toluidine Blue. Ultrathin sections were processed according to standard techniques.

For histochemical investigations, animals were perfused with Bouin's solution diluted 1:4 in PBS. After dissection of individual organs and dehydration, embedding was performed in low melting point paraffin (Wolff, Germany). Serial sections (7 μm) were cut and mounted on glass slides covered with Biobond (British Biocell, London, UK). Central sections of each series were stained with Haematoxylin and Eosin for standard light microscopy. Correlative sections of all tissues were stained for lysosomal marker antigens

cathepsin D (Kasper et al., 1996) and lysosomal-associated-membrane protein type I (DSHB, University of Iowa, USA). Detection of primary antibody binding was performed by the use of biotin-labelled secondary antibodies and either avidin-biotin complexes or tyramide signal amplification.

### Light and electron microscopy of bone

Calvariae, tibiae and femora of 12 animals (three of each genotype) were fixed for 36 hours in 4% formaldehyde and 1% glutaraldehyde in 0.1M sodium cacodylate buffer (pH 7.4). After rinsing in buffer, the material was post-fixed in 1% osmium tetroxide dehydrated in ethanol and embedded in LX-112 (Ladd Research Industries, Burlington, USA). Ultrathin sections were prepared, stained and examined in a Zeiss EM 10C electron microscope. Part of the tissue samples was fixed in 4% formaldehyde in 0.1 M sodium cacodylate buffer, dehydrated and embedded in LR White. Semi- and ultrathin sections were incubated with goat anti-rat osteopontin (Dr W. Butler, Houston, TX) (McKee and Nanci, 1996), mouse-anti osteocalcin (kindly provided by Dr P. Cloos of OsteoMeter, Herlev, DK) or biotinylated sWGA (Vector Lab., Burlingame, CA). The sections were incubated with protein A-gold (Aurion, Wageningen, NL), Histomouse-SP Kit of Zymed Laboratories (San Francisco, CA) or extravidin-gold (Sigma), respectively. For light microscopic immunolocalisation, the signal was silver enhanced (Aurion, Wageningen, NL).

### Scanning electron microscopy

Bones fixed in 70% ethanol were dehydrated in ethanol and embedded in PMMA. Trimmed blocks were micro-milled (Reichert-Jung UltraMiller, Leica UK) and carbon coated and imaged using backscattered electrons (BSE; 20kV, Zeiss DSM962). The same blocks were later oxygen plasma ashed (PlasmaPrep 100, Nanotech, UK; to remove carbon, PMMA, cells and any non-mineralised matrix, and expose mineralised cartilage and bone) and again coated with carbon and imaged with BSE.

### EDX-analysis of bone crystals

Ultra-thin sections of non-decalcified calvarial bone of LAP/Acp5 knockout mice were collected on carbon-coated grids. The sections were not counterstained and element analysis was performed with an EDX apparatus attached to a Philips CM12 electron microscope.

### Hydrolysis of osteopontin and immunoblotting

Long bones were removed from feshly killed six month old mice and dissected free of muscle. The bones were minced and homogenised in 0.4 M sodium acetate, pH 5.6 containing 1% w/v Triton X-100. Recombinant mouse osteopontin (R&D Systems, Wiesbaden, Germany; 600 ng) was incubated with 50 μg of bone extracts corresponding to about 4 mU of tartrate-resistant acid phosphatase activity in extracts from control bones in 200 mM sodium acetate buffer, pH 5.6 at 37°C for times ranging from 1 to 3 hours. Control tubes of enzyme and osteopontin alone were set up in the same buffer. At the end of the incubation period, aliquots containing the equivalent of 300 ng osteopontin were analysed by SDS-polyacrylamide gel electrophoresis and immunoblotting with antibodies to osteopontin (R&D Systems) or anti-phosphoserine (Chemicon, Hofheim, Germany). Hydrolysis of osteopontin was also carried out in the presence and absence of inhibitor compounds, molybdate, L-tartrate, vanadate at 10 mM and proteinase inhibitor cocktail (Boehringer Mannheim, FRG).

## RESULTS

### Generation of mice doubly deficient for LAP and Acp5

The lack of detectable morphological signs of lysosomal storage material in most tissues of LAP-deficient mice (Saftig et al., 1997) pointed to the existence of compensating pathways for the metabolism of phosphate esters in lysosomes. After subcellular fractionation of LAP-deficient liver tissues by Percoll density centrifugation, fractions enriched in markers for lysosomes contained residual tartrate-resistant acid phosphatase activity. Partial purification of the tartrate-resistant activity and further biochemical characterisation using different effectors as well as immunoprecipitation with an antibody specific for uteroferrin/Acp5 suggested that Acp5 was the principal candidate for compensating the loss of LAP (data not shown).

To investigate if LAP and Acp5 indeed compensate for each other we generated mice that were deficient for both enzymes. For this purpose $Lap^{-/-}$ animals were bred with $Acp5^{-/-}$ animals to yield LAP/Acp5 doubly heterozygote mice ($Lap^{+/-}/Acp^{+/-}$). Genotyping was carried out using established Southern blot protocols to demonstrate the null-alleles for *Lap* and *Acp5* (Saftig et al., 1997; Hayman et al., 1996) (Fig. 1A). Breeding of animals homozygote deficient for one gene and heterozygote for the other gene (e.g. $Lap^{-/-}$; $Acp5^{+/-}$) resulted in 23% (15 out of 66) mice which were deficient for both genes. This frequency was close to that expected for Mendelian inheritance.

To test for expression of LAP and Acp5, northern blot analyses (not shown) and acid phosphatase enzyme assays of Percoll gradient-enriched lysosomal fractions of liver tissues were performed. L-tartrate-sensitive acid phosphatase activity was undetectable in lysosomal fractions from LAP-deficient and doubly deficient animals (Fig. 1B). Tartrate-resistant Acp5 activity was determined in the immunoprecipitates obtained from lysosomal extracts with an Acp5 (uteroferrin) -specific antibody. No tartrate resistant activity was detectable in the resuspended immunoprecipitates from Acp5 single and doubly deficient animals, while considerable Acp5 activity was observed in those from control and LAP-deficient mice (Fig. 1B). Thus, all tartrate-sensitive and tartrate-insensitive acid phosphatase activity towards *p*-nitrophenol-phosphate in liver is represented by Acp5 and LAP, respectively, and was lacking in doubly deficient mice. In addition, subcellular fractionation experiments of LAP/Acp5-deficient kidney and spleen tissues failed to demonstrate the existence of other lysosomal *p*-nitrophenyl-phosphate cleaving activities (not shown).

### Progressive hepatosplenomegaly in LAP/Acp5 doubly deficient mice

LAP/Acp5 deficient animals are viable and fertile. Like Acp5 single knockout mice, LAP/Acp5 doubly deficient mice weigh about 10-15% lower than control or LAP-deficient mice (data not shown). Although LAP- and Acp5 single knockouts can not be distinguished from controls, the doubly deficient animals can easily be recognised. They display a blown up, ball-like trunk and gait disturbances. LAP/Acp5 deficient mice also have an increased mortality. By 17 months, about half of the double knockout mice had died, whereas the mortality of single knockout mice was like that of control mice (Fig. 1C). LAP/Acp5 deficient mice revealed severe enlargement of liver and spleen (Fig. 1D), filling up most of the abdominal cavity. The extent of the hepatosplenomegaly varied between animals, but showed a clear progression with age (Fig. 1E,F). In mice of 1 year of age or older, the liver contributed up to 25% of the

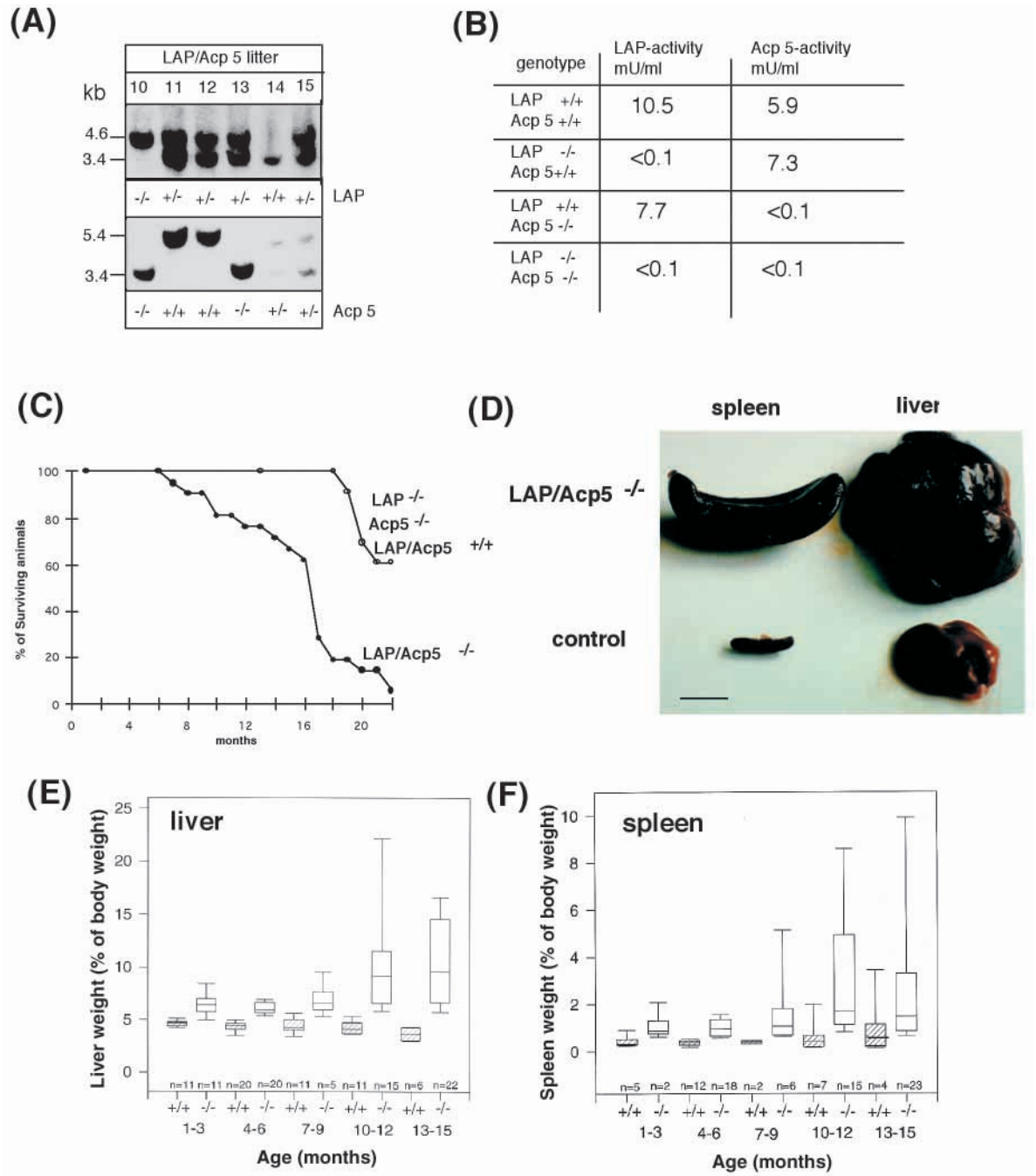


**Fig. 1.** (A) Generation of LAP/Acp5 doubly deficient mice. Southern blot with external probes for the targeted LAP locus (Saftig et al., 1997) and the Acp5 locus (Hayman et al., 1996). (B) Determination of lysosomal acid phosphatase activity (Waheed et al., 1985) in enriched lysosomal liver fractions of control, single deficient and doubly deficient mice. Acp5 activity was determined after immunoprecipitation with an anti-uteroferrin antibody. (C) LAP/Acp5 doubly knockout mice display an increased mortality starting at about 8 months of age. The results from LAP and Acp5 single knockout as well as control animals are also shown. (D) Hepatosplenomegaly in LAP/Acp5 deficient animal. The spleen and liver of an extreme case of hepatosplenomegaly in LAP/Acp5 knockout animals is shown. (E) Progressive increase in liver weight in LAP/Acp5-deficient mice. A box blot of control (striped boxes) and LAP/Acp5 deficient liver weights is shown from 1-15 month of age. (F) Progressive increase in spleen weight in LAP/Acp5-deficient mice. A box plot of control (striped boxes) and LAP/Acp5 deficient spleen weights is shown from 1-15 month of age.

total body weight when compared with 4% in controls. The spleen of 1-year-old mice was about two- to threefold larger than in controls. Hepatosplenomegaly was never observed in LAP- and Acp5 single knockout mice.

Analysis of LAP/Acp5-deficient serum revealed unchanged levels of electrolytes (e.g. iron and phosphate), α-amylase, alkaline phosphatase, urea and glutamate-oxalacetate-transaminase. The number of white blood cells increased about twofold in LAP/Acp5-deficient mice at the age of 12-14 months, whereas the number of erythrocytes,

haematocrit and concentration of haemoglobin decreased only slightly (data not shown).

### Lysosomal storage in liver and spleen in LAP/Acp5 deficient mice

Control, LAP-deficient, Acp5-deficient and LAP/Acp5-deficient animals were analysed morphologically at ages between 1.5 and 10 months. Light microscopical examination revealed signs of lysosomal storage in liver (Fig. 2B) and spleen (Fig. 2D) of LAP/Acp5 deficient mice but not of single knockouts and controls (Fig. 2A,C). Cells in kidney (Fig. 2F), liver and spleen (not shown) of the double knockout showed high levels of the lysosomal marker antigens LAMP1 (lysosome-associated membrane protein 1) and cathepsin D (not shown) compared with the other genotypes (Fig. 2E; shown for control kidney).

In LAP/Acp5 deficient liver, a remarkable increase with the macrophage specific markers F4/80 and MHC class II was also observed (not shown). It was notable that staining with succinylated wheat germ agglutinin (sWGA) and peanut agglutinin (PNA) resulted in a pronounced staining reaction of Kupffer cells (Fig. 2H for sWGA), which was not observed in singly-deficient mice and controls (Fig. 2G).

Ultrastructural analysis of LAP/Acp5-deficient liver revealed accumulation of vacuoles in hepatocytes in the vicinity of bile ducts (Fig. 3A). Lysosomal storage vacuoles were also frequently found in Kupffer cells (Fig. 3B,C). A prominent vacuolisation was also observed in macrophages (Fig. 3D) and sinus endothelium (Fig. 3E) of the spleen. In addition, in fibroblasts of the liver (not shown) and kidney (Fig. 3f), accumulation of lysosomal storage vacuoles were observed. These alterations were not observed in cells of single knockouts and controls (Table 1). The cytoplasmic vacuoles in the doubly deficient tissues were membrane limited and appeared either empty or contained material of low electron density (Fig. 3C,D).

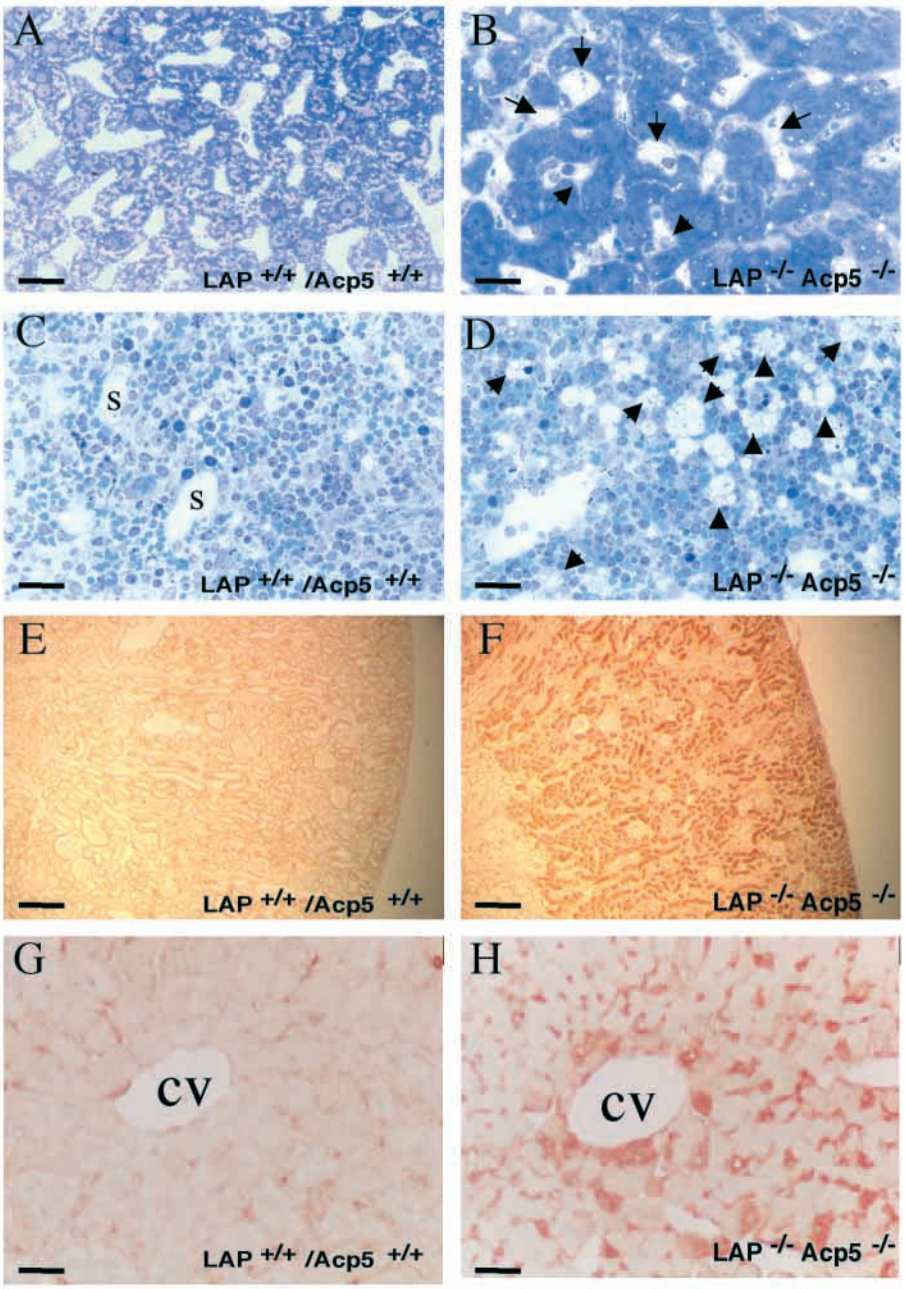


**Fig. 2.** Lysosomal storage in LAP/Acp5-deficient liver, spleen and kidney. (A,B) Semithin section of a liver of a 3.5 month old control (A) and LAP/Acp5-deficient (B) mouse. Vacuolated Kupffer cells are indicated by arrows. (C,D) Sections through a control and LAP/Acp5-deficient spleen. Numerous vacuolated macrophages are apparent in the double deficient mouse (arrowheads in D); S, sinus. (E,F) LAMP1 immunohistology of control (E) and LAP/Acp5-deficient (F) kidney, demonstrating an increased immunoreactivity in LAP/Acp5-deficient kidney. (G,H) Lectin staining (sWGA) of control (G) and LAP/Acp5-deficient liver (H); cv, central vein. Note the increased labelling of LAP/Acp5-deficient Kupffer cells. Scale bars: 15 μm in A,B; 25 μm in C,D; 400 μm in E,F; 30 μm in G,H.

In 3- to 6-month-old LAP/Acp5-deficient mice, the number of Kupffer cells after liver perfusion and Kupffer cell isolation was about 12.4 (±2.9) × $10^6$ cells/ liver compared to 5.9 (±2) × $10^6$ cells/ liver in controls. The number of LAP/Acp5-deficient Kupffer cells increased to 109 (±24.5) × $10^6$ cells/liver in 9-12 month old mice compared with about 9 (±3.1) × $10^6$ cells/liver in controls. The number of hepatocytes also increased in parallel to about 1.8 fold in LAP/Acp5 doubly deficient animals of 6 month of age. It appears that an increased number of hepatocytes, but particularly of Kupffer cells, contributes to the increase in liver size. The latter cell type is also characterised by a hypertrophic appearance (Fig. 3C,D), which may also contribute to the enlarged organ size.

### Lysosomal storage pathology in other tissues of LAP/Acp5 deficient mice

Light microscopic examination of brain and kidney of LAP/Acp5 doubly deficient mice revealed the presence of lysosomal storage in subsets of microglial, astroglial and ependymal cells of the brain and in ependymal cells and podocytes of the kidney. Lysosomal storage in these cells has also been noted in LAP-single knockout mice (Saftig et al., 1997). In doubly deficient mice, however, the storage lysosomes developed much earlier. The storage seen in one month old mice was comparable with that in 6-month-old LAP-singly deficient mice. Lysosomal storage vacuoles were additionally observed in LAP/Acp5-deficient mice in other cells of the kidney (cortical peritubular fibroblasts and macrophages), bone (osteocytes), and peripheral and central nervous systems (Table 1). Additionally, a prominent vacuolisation was observed in a number of bone marrow cells (not shown). Such alterations were not observed in cells of single knockouts and controls.

### Bone abnormalities in LAP/Acp5 deficient mice

The staggering gait of LAP/Acp5 doubly deficient mice prompted further examination of their skeletal system. The bone abnormalities previously described for Acp5-deficient animals (Hayman et al., 1996) and LAP-deficient animals (Saftig et al., 1997) were also observed in the doubly deficient mice, but it appeared that the bone malformations are in some aspects more severe than in single knockouts. Most evident is the foreshortening of long bones, especially of femur and tibia (Fig. 4A-D, Table 2). In addition the doubly deficient mice displayed a foreshortened and narrower skull with a higher vault, presumably a compensatory change to accommodate brain growth (not shown).

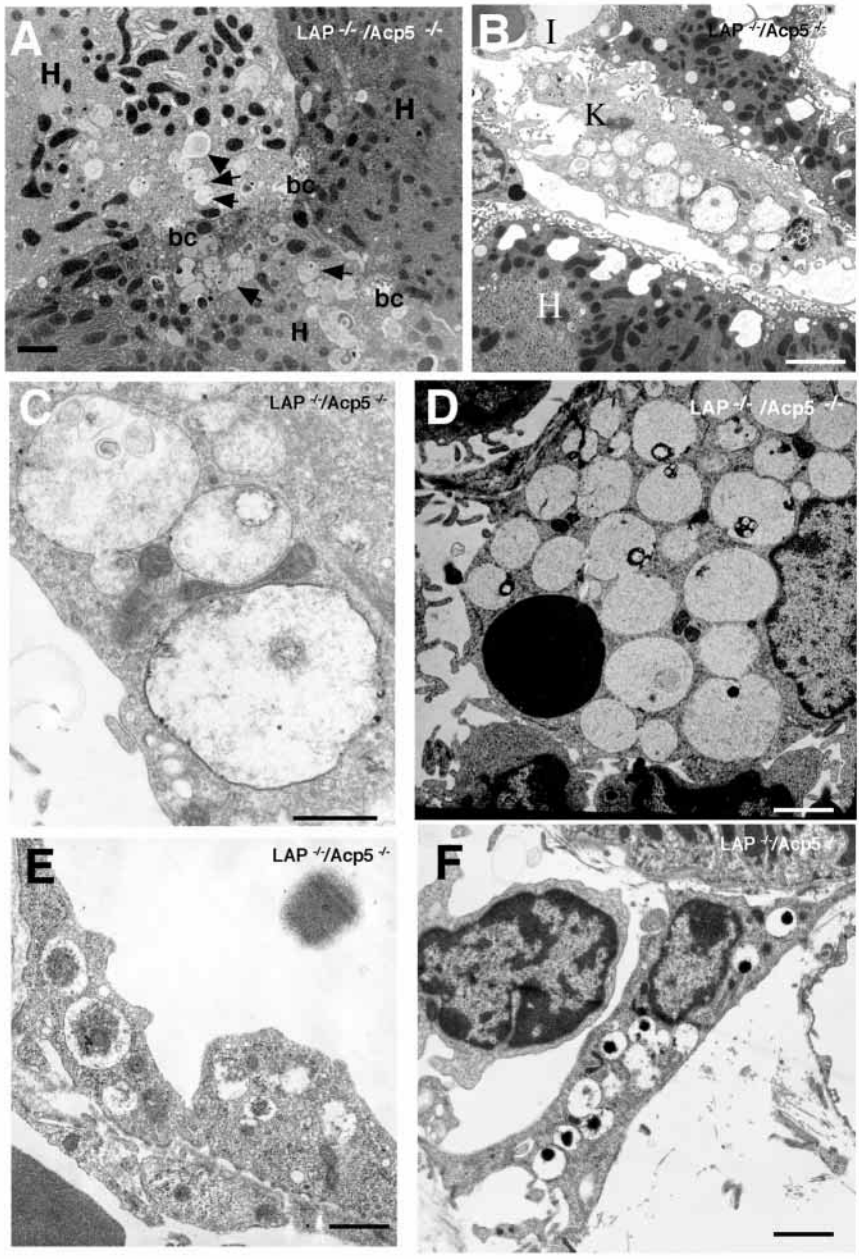


**Fig. 3.** Electron microscopy of: (A) storage lysosomes (arrows) in hepatocyte in the vicinity of a bile canaliculus of a 6-month-old LAP/Acp5 deficient mouse (H, hepatocyte; bc, bile canaliculus); and (B) Kupffer cell (K) with storage lysosomes (I, Ito cell). (C) Higher magnification of storage lysosomes in a LAP/Acp5-deficient Kupffer cell. (D) LAP/Acp5-deficient spleen macrophage filled with storage lysosomes. (E) Sinus endothelial cell of a LAP/Acp5-deficient spleen with storage vacuoles (F) LAP/Acp5-deficient kidney fibroblast filled with storage vacuoles. Scale bars: 1.4 μm in A; 3.5 μm in B; 0.8 μm in C; 2.4 μm in D; 3.0 μm in E; 4.5 μm in F.

Microscopical examination of bone sections (Fig. 4E-H) showed expansion of the cartilaginous growth plates with disruption, hyperplasia and hypertrophy of chondrocytes. These alterations were most pronounced in LAP/Acp5-deficient mice. Also using BSE SEM, growth plates of $Acp5^{-/-}$ and $LAP/Acp5^{-/-}$ bones proved abnormal with a thicker zone of unmineralised cartilage and a thinner zone of mineralised cartilage (Fig. 4I,J). The chondrocyte lacunae (and, presumably the chondrocytes) were larger in the mineralised cartilage zone. In all four genotypes, resorption had occurred of both bone and calcified cartilage. Thus, while resorption may be impaired in the Acp50deficient and double knockout mice (as in vitro resorption experiments also showed), it is not prevented even in the absence of both LAP and Acp5. Modelling by subperiosteal resorption in the metaphyseal region was present, as well as endosteal resorption. In vitro bone formation studies using osteoblasts from the double knockout indicated that they functioned as well as the controls (data not shown).

Staining with the lectin succinylated wheat germ agglutinin (sWGA) demonstrated reactive extracellular material (cartilage) in LAP/Acp5 deficient growth plates, whereas such a staining pattern was not observed in control and single knockout mice (Fig. 4K,L). Alizarin Red- and Alcian Blue-

**Table 1. Distribution of lysosomal storage in phosphatase-deficient mice**

| Tissue/genotype | *Lap*$^{-/-}$ | *Acp5*$^{-/-}$ | *Lap*/*Acp5*$^{-/-}$ |
|---|---|---|---|
| Liver | – | – | Kupffer cells +++<br>Fibroblasts +<br>Venous endothelium +<br>Hepatocytes + |
| Spleen | – | – | Macrophages +++<br>Sinus-endothelial cells +<br>Reticulum cells + |
| Kidney | Podocyte (+)<br>Intermediate tubuli (+) | – | Podocytes ++<br>Intermediate tubuli (+)<br>Fibroblasts ++<br>Macrophages +++ |
| Bone marrow | – | – | Macrophages +++<br>Sinus-endothelial cells + |
| Brain | Glia ++<br>Ependym ++ | – | Glia ++<br>Ependym ++ |
| Bone | Osteoclasts ++ | Osteoclasts + | Osteoclasts +++ |

(+), storage in some cells; +, storage in all cells; ++, strong storage in all cells; +++, very strong storage in all cells.

stained preparations of 7 and 18 days old animals did not reveal differences in overall bone or cartilage distribution between the genotypes (not shown).

Ultrastructural analysis of long bones and calvariae of single and double knockout mice revealed that the overall morphology was similar to control bones. In osteoclasts of the knockout mice, however, intracellular vacuoles containing fine filamentous material of moderate electron density were frequently seen (Fig. 5A). These vacuoles resembled lysosomal structures. In the Acp5-deficient osteoclasts these vacuoles proved to contain, in addition, linear features that resembled mineral crystallites (Fig. 5B). In doubly deficient osteoclasts, similar vacuoles but with more such features were observed (Fig. 5C,D). It is not clear from the TEMs whether these are crystals per se, or crystal associated matrix (‘crystal ghosts’). Crystallite profiles were not observed in the vacuoles of the LAP-deficient cells. Subsequent energy dispersive X-ray emission microanalysis (EDX) of 0.1 μm sections in the TEM showed the presence of Ca and P peaks at these locations, indicating that these linear features are likely to be bone crystals. Quantitative analysis of the vacuoles (with or without crystallite profiles) is shown in Table 3 and demonstrates that the highest number of vacuoles with these features is present in the doubly deficient osteoclasts.

Acp5 has been found to dephosphorylate osteopontin in vitro (Ek-Rylander et al., 1994; Andersson and Ek-Rylander, 1995). Immunolocalisation of osteopontin at light and electron

**Table 2. Foreshortening of long bones in phosphatase deficient mice**

| | Control (+/+) | *Lap*$^{-/-}$ | *Acp5*$^{-/-}$ | *Lap*$^{-/-}$/*Acp5*$^{-/-}$ |
|---|---|---|---|---|
| Femur | 15.4±0.5 | 15.2±0.1 | 12.5±0.5 | 10.7±0.4 |
| Tibia | 16.7±0.4 | 16.9±0.1 | 14.4±0.2 | 13.7±0.3 |
| Humerus | 11.1±0.2 | 11.5±0.1 | 9.6±0.2 | 9.0±0.2 |

Long bones (femora, tibiae, humeri) of six 3-month-old male mice were dissected free of soft tissues and bone length was measured with fine callipers. The mean length in mm and standard error (±s.e.m., $n$=6) are given.

**Table 3. Vacuoles in the cytoplasm of osteoclasts**

| | Vacuoles | |
|---|---|---|
| | Vacuoles per cell | Mineral content |
| Control$^{+/+}$ | 0 | – |
| *Lap*$^{-/-}$ | 1.9±0.6 | – |
| *Acp5*$^{-/-}$ | 0.6±0.6 | + |
| *Lap*$^{-/-}$/*Acp5*$^{-/-}$ | 2.8±0.3 | + |

Values represent mean (±s.e.m.). All vacuoles contain fine filamentous material of moderate electron density.

microscopic levels revealed the presence of this protein in the resorption zone adjacent to the osteoclast (Fig. 6). High levels of osteopontin were found adjacent to Acp5 and LAP/Acp5 doubly deficient osteoclasts (Fig. 6B,C,F,G), whereas osteopontin labelling was low or even absent in the resorption zone of LAP-deficient and control osteoclasts (Fig. 6A,D,E). Quantitative analysis revealed a high level of osteopontin staining adjacent to 11% of control osteoclasts, 23% of *Lap*$^{-/-}$ osteoclasts, 40% of *Acp5*$^{-/-}$ osteoclasts and 84% of *Lap*/*Acp5*$^{-/-}$ osteoclasts. In the double knockout osteoclasts, osteopontin was frequently found in the electron dense vacuoles described above (Fig. 6G). No intracellular labelling was seen in control and LAP deficient osteoclasts. The overall expression of osteopontin in long bones was not significantly different in LAP/Acp5 deficient mice when compared to the other genotypes.

In addition, we immunolocalised osteocalcin, a non-collagenous protein that is not phosphorylated. In contrast to osteopontin, no accumulation of this protein was found in the resorption zone of osteoclasts (data not shown).

To further strengthen the role of osteopontin processing by both LAP and Acp5, we have incubated recombinant osteopontin with bone extracts from control and LAP/Acp5-deficient mice. Immunoblot analysis using antibodies to osteopontin showed that the osteopontin bands diminished upon incubation with extracts from control bones. By contrast, incubation of osteopontin with LAP/Acp5 deficient bone extracts did not result in a reduction of osteopontin immunoreactivity (Fig. 7A). Incubation of the same blot with antibodies directed against anti-phosphoserine demonstrated that the osteopontin-specific band seen in Fig. 7A represented the phosphorylated form of this protein. After incubation with control bone extracts, these bands disappeared because of dephosphorylation. This process is severely reduced in bone extracts derived from LAP/Acp5-deficient animals (Fig. 7B). The presence of proteinase inhibitors during incubation had no effect on the disappearance of bands, giving further proof to the fact that the loss of immunoraectivity is due to dephosphorylation. Known inhibitors of LAP (L-tartrate) and Acp5 (molybdate) could almost completely prevent the dephosphorylation of osteopontin when incubated with extracts of control bones (Fig. 7C).

Immunoblot and N-terminal sequencing of bone extracts revealed an increased amount of bone-sialoprotein (BSP) and chondrocalcin in LAP/Acp5-deficient bones (not shown). Interestingly, labelling with sWGA was very high in the mid-portion of calvarial bone, whereas the labelling was much lower in single knockout and control bones in LAP/Acp5-deficient bone (not shown), indicating a role of both

phosphatases in bone formation and remodelling for which they can substitute each other.

### Normal dephosphorylation of mannose 6-phosphate residues in LAP/Acp5 deficient fibroblasts

Earlier studies have indicated that dephosphorylation of mannose 6-phosphate residues from lysosomal enzymes occurs in the late endocytic compartment (Bresciani et al., 1992). This phosphatase was shown to be distinct from LAP and presumed to be Acp5 (Bresciani and von Figura, 1996). LAP/Acp5-deficient embryonic fibroblasts were used to determine if dephosphorylation of mannose 6-phosphate residues from lysosomal enzymes is altered in the absence of the two known lysosomal phosphatases. Our data demonstrate, however, that LAP/Acp5 fibroblasts were, like control cells, readily able to dephosphorylate $^{32}$P-labelled arylsulfatase A that had been endocytosed (Fig. 8). These findings suggest that yet another unknown phosphatase may compensate for the lack of LAP/Acp5 activity.

## DISCUSSION

If LAP is crucial for the catabolism of one or several phosphorylated substrates, we reasoned that deficiency of LAP would cause an accumulation of these substrates in lysosomes (Saftig et al., 1997). Despite the ubiquitous expression of LAP in normal mice, lysosomal storage could not be detected in the majority of tissues of LAP-deficient mice. The lack of detectable morphological signs of lysosomal storage suggested that the function of LAP in many tissues may be compensated by other phosphatases of the lysosomal compartment. Accordingly, we found at least one additional acid phosphatase activity in lysosomal fractions of LAP-deficient tissues. Biochemical characterisation of this activity in LAP-deficient liver revealed a striking similarity with tartrate-resistant acid phosphatase activity type 5 (TRAP or Acp5). Acp5 has been described to be a lysosomal phosphatase but is predominantly expressed in cells of the monocyte/phagocyte system, i.e. alveolar macrophages, Kupffer cells and osteoclasts (Drexler and Gignac, 1994;

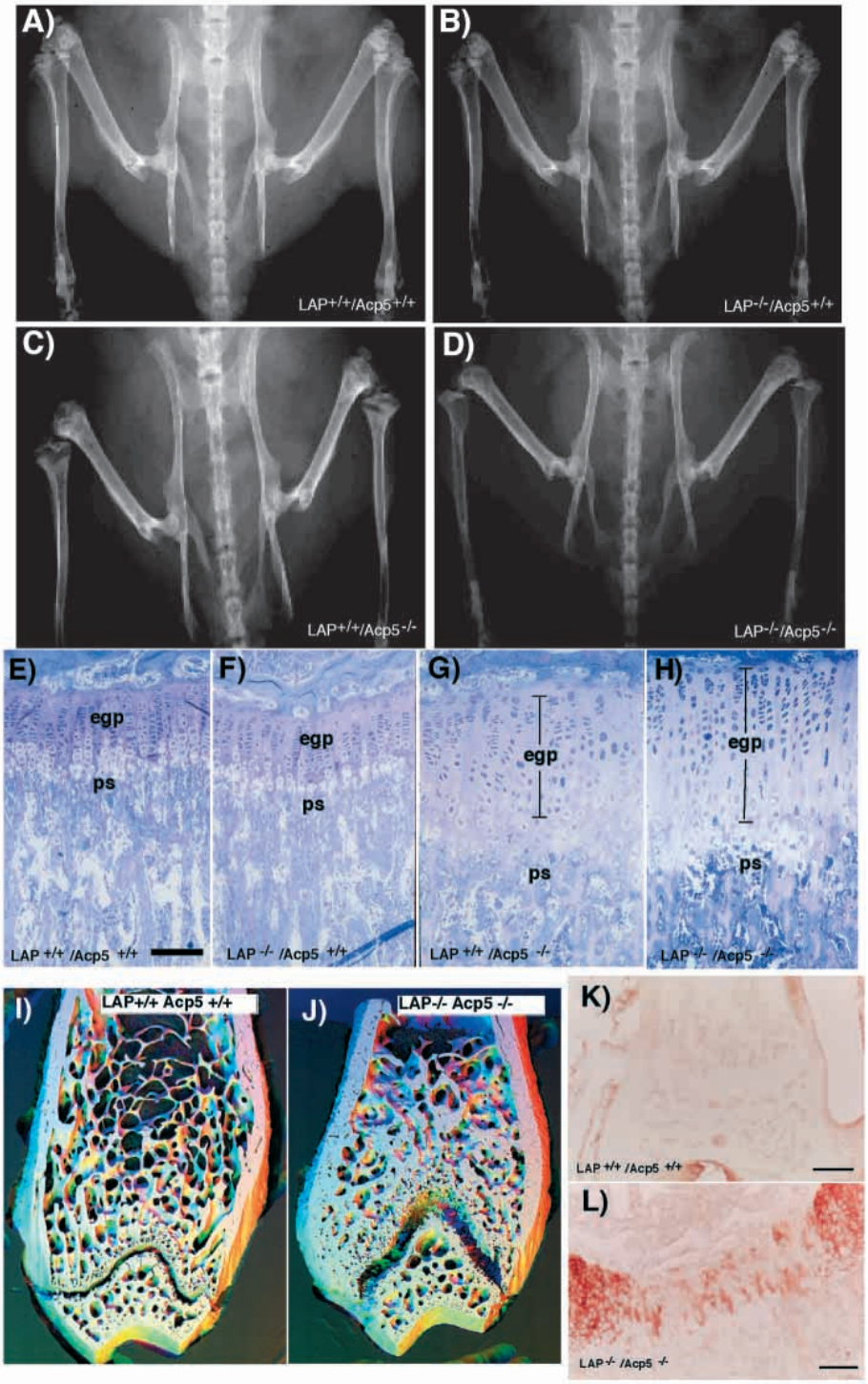


**Fig. 4.** Bone abnormalities in LAP/Acp5-deficient mice. (A-D) Radiographs of 8-week-old mice: (A) control; (B) *Lap*$^{-/-}$; (C) *Acp5*$^{-/-}$; and (D) *Lap*$^{-/-}$/*Acp5*$^{-/-}$. Note the foreshortening of long bones in the LAP/Acp5-deficient mouse. (E-H) Light microscopy of growth plates of 3-month-old mice: (E) control; (F) *Lap*$^{-/-}$; (G) *Acp5*$^{-/-}$ and (H) *Lap*$^{-/-}$/*Acp5*$^{-/-}$. Note the expansion of the cartilaginous growth plates (egp) in Acp5- and LAP/Acp5-deficient mice with disruption, hyperplasia and hypertrophy of the chondrocytes (ps, primary spongiosa). (I,J) PMMA embedded distal femurs of control and *Lap*$^{-/-}$/ *Acp5*$^{-/-}$ after plasma ashing. Imaged with three detectors, used to give red, green and blue signal components. Colour here codes for direction and slope of the internal surfaces exposed by removing PMMA. Control image field is 4 mm in height. (K,L) Localisation of succinylated wheat germ agglutinin (sWGA)-binding sites in growth plates of (K) control bone and (L) LAP/Acp5 doubly deficient bone. Scale bars: 120 μm in E-H; 50 μm in K,L.

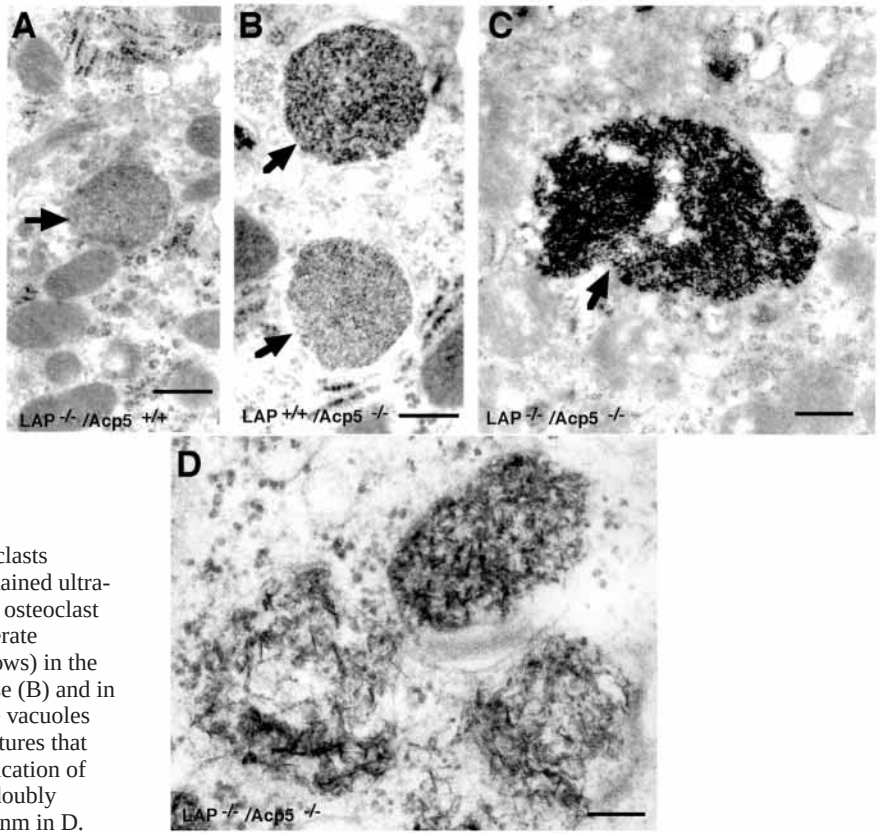


**Fig. 5.** Vacuolisation of phosphatase-deficient osteoclasts shown in TEM of post-osmicated, uranyl and lead stained ultra-thin sections. (A) Intracellular vacuole (arrow) in an osteoclast of a LAP-deficient mouse. Note the content of moderate electron density of the vacuole. (B,C) Vacuoles (arrows) in the cytoplasm of an osteoclast of a Acp5-deficient mouse (B) and in an osteoclast from a doubly deficient mouse (C): the vacuoles have a higher electron density and contain linear features that may represent mineral crystallites. (D) High magnification of typical mineral cystallites containing vacuoles of a doubly deficient osteoclast. Scale bars: 0.5 μm in A-C; 130 nm in D.

Yaziji et al., 1995). Immunoprecipitation of the tartrate-resistant activity with an Acp5-specific antibody confirmed that Acp5 represents the acidic phosphatase activity found in LAP-deficient liver lysosomal fractions.

## Lysosomal storage in soft tissues of LAP/Acp5 double knockout mice

To evaluate if Acp5 indeed compensates for the loss of LAP in different tissues of LAP-deficient mice, animals were generated that are deficient for both known lysosomal acid phosphatases. The different phenotypes of LAP and Acp5 singly deficient mice indicate that the two lysosomal phosphatases are crucial for the catabolism of at least some distinct substrates. However, mice deficient in either of the two phosphatases show a relatively mild phenotype. Double knockouts, on the other hand, display a more severe phenotype (e.g. hepatosplenomegaly, bone abnormalities), which is more than a mere addition of the alterations seen in singly deficient animals. Kupffer cells, for example, appear normal in single deficient mice, but show excessive lysosomal storage in the doubly deficient mice. This strongly suggests that LAP and TRAP can substitute for each other for a number of substrates and the accumulation of such common substrates can therefore be observed only if both lysosomal phosphatases are deficient. In addition several LAP-specific alterations, such as microglial activation and MHC-II upregulation (Saftig et al., 1997), occurred at a much earlier age in the doubly deficient mice than in LAP-singly deficient mice. Thus, for several substrates, the two phosphatases can only partially substitute for each other.

The reason for the observed hepatosplenomegaly in LAP/Acp5-deficient animals remains to be explained. One might speculate that the lysosomal storage observed in Kupffer cells, in hepatocytes of LAP/Acp5 knockout animals, as well as storage in spleen macrophages of the red pulp contributes to the increase in size and weight of the organs. The lysosomal storage is progressive and accompanied by an increase in number of hepatocytes and Kupffer cells. Similar pathological alterations in liver and spleen have also been described for individuals suffering from Gaucher and Niemann-Pick disease (Nyhan and Ozand, 1998). In addition, a defective liver perfusion may cause a high local blood pressure and backflow into the spleen contributing to the increased organ size.

Isolation of a sufficient number of Kupffer cells should allow a biochemical characterisation of the lysosomal storage material, in order to elucidate the nature of the hitherto unknown physiological substrates degraded by both lysosomal phosphatases. It is of note that Kupffer cell lysosomes, as well as the peribiliary bodies of hepatocytes, have been shown to contain an elevated level of phosphorus (Köpf-Maier, 1990). Preliminary attempts to isolate lysosomes of Kupffer cells from doubly deficient mice turned out to be unsuccessful because of their fragility, which caused disruption even under the mildest possible condition for their isolation.

## Alterations in mineralised tissues of LAP/Acp5 doubly deficient mice

Phosphorylated proteins such as osteopontin and bone sialoprotein play an important role in mineralisation. Our data suggest that processing of these proteins was disturbed in phosphatase-deficient mice. Mineralisation of cartilage and

bone, as well as degradation of these compounds proved to be altered in these mice.

A defective endochondral ossification with delayed mineralisation of the cartilage was observed in 6- to 8-week-old mice with a deficiency of Acp5. Osteopetrosis with increased mineralisation of bone tissue was observed in older mice (Hayman et al., 1996). In doubly deficient animals, bone pathology appeared to be somewhat more severe compared with Acp5 singly deficient mice, in terms of an increased foreshortening of long bones, morphological alterations of the growth plate and lysosomal storage in osteoclasts. The rather mild osteopetrotic phenotype in Acp-5 single knockout mice (Hayman et al., 1996) may be explained by a partial compensation by LAP.

Our data are the first to provide evidence for the view (Flores et al., 1992; Ek-Rylander et al., 1994) that acid phosphatases, in particular Acp5, are involved in processing non-collagenous proteins (e.g. osteopontin) by osteoclasts during bone resorption. We demonstrate that high levels of osteopontin are present adjacent to actively resorbing osteoclasts in the absence of these enzymes. This finding strongly suggests that the lack of Acp5 causes a hindered degradation of osteopontin resulting in an accumulation of this protein in the resorption zone. Alternatively, it is possible that synthesis of osteopontin by osteoclasts had increased owing to the lack of phosphatases. This is not very likely, however, as the protein was also found intracellularly in lysosome-like vacuoles that contained features resembling mineral crystallites. The EDX analysis supports the view that they represent bone crystals. The colocalisation of mineral crystallites and osteopontin suggests the uptake of these components by the osteoclast.

The severely reduced ability of LAP/Acp5-deficient bone extracts to dephosphorylate recombinant mouse osteopontin in vitro adds further support to the hypothesis that the phosphatases are involved in the dephosphorylation of this protein in vivo.

We propose that dephosphorylation of non-collagenous proteins, e.g. osteopontin, does not occur because of the lack of Acp5 activity, and that this dephosphorylation is essential for proper solubilisation of the mineral crystallites. The combined presence of a low pH and Acp5 under normal conditions is thus assumed to result in an efficient processing of specific non-collagenous proteins and minerals. After this activity, which occurs primarily in the extracellular resorption area, some proteins or their fragments are taken up by the osteoclast and subsequently further digested in the lysosomal apparatus. The latter digestion appears to involve activity of LAP, as we show that its deficiency results in an accumulation of material in cytoplasmic vacuoles.

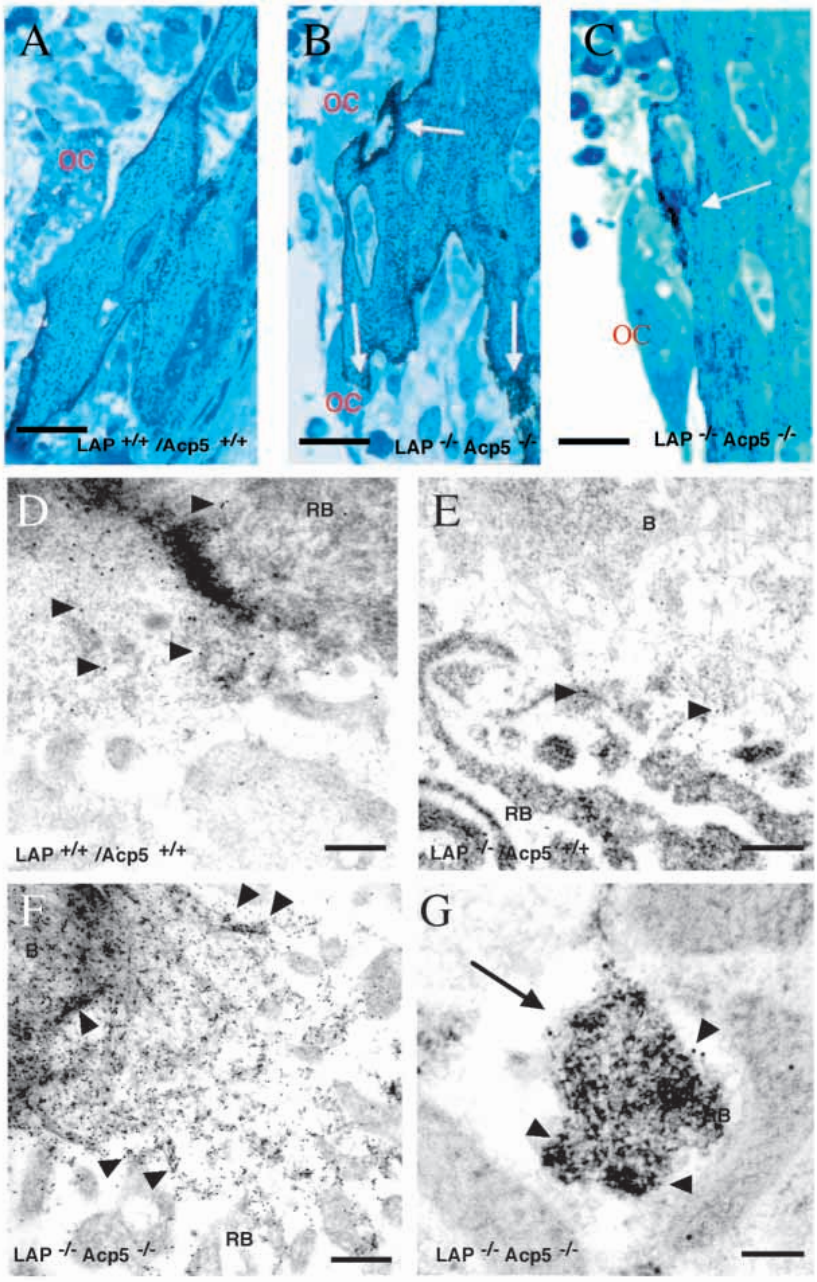


**Fig. 6.** (A-C) Immunolocalisation of osteopontin in bones. Light microscopic localisation by silver enhancement. (A) Osteopontin localisation in long bone of a control mouse. Note labelling in the bone matrix and the cement lines. Adjacent to the ruffled border of the osteoclast (OC) a low level of label is apparent. (B,C) Localisation of osteopontin in long bone of a doubly deficient mouse. A high level of labelling (arrows) is seen adjacent to the ruffled border of the osteoclast. (D-G) Electron microscopic localisation of osteopontin in bones. (D) Ruffled border area (RB) of an osteoclast of a control mouse. Gold particles (arrowheads) indicate the presence of osteopontin in the bone matrix at some distance from the ruffled border. (E) Ruffled border area of an osteoclast of a LAP-deficient mouse. Note the presence of a small number of gold particles (arrowheads) adjacent to the ruffled border membrane (B, bone). (F) Ruffled border area of an osteoclast of a LAP/Acp5 doubly deficient mouse. A large number of gold particles (arrowheads) are seen adjacent to the ruffled border membrane. (G) Intracellular vacuole (arrow) in an osteoclast of a doubly deficient mouse. The presence of osteopontin in the vacuole is indicated by a high number of gold particles (arrowheads). Scale bars: 20 μm in A-C; 0.18 μm in D; 0.25 μm in E,F; 0.15 μm in G.

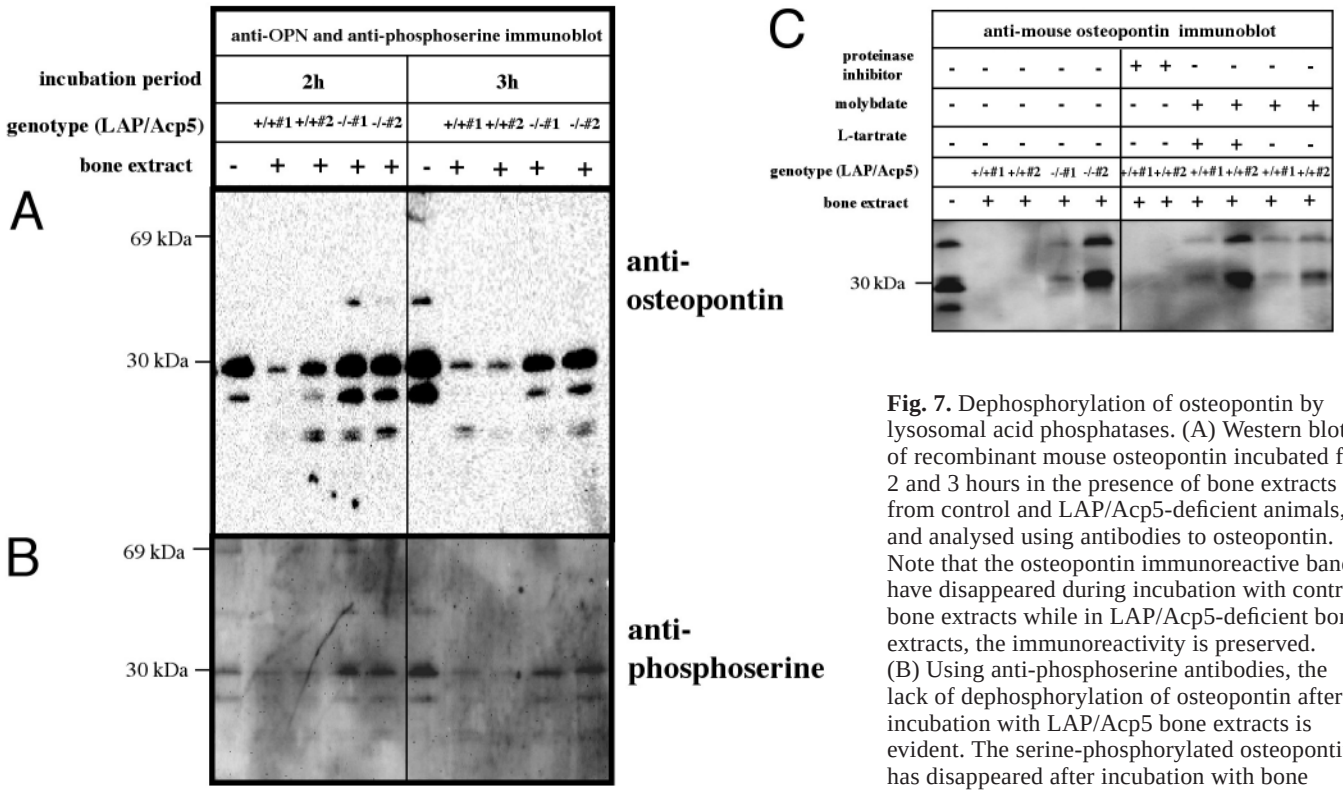


**Fig. 7.** Dephosphorylation of osteopontin by lysosomal acid phosphatases. (A) Western blot of recombinant mouse osteopontin incubated for 2 and 3 hours in the presence of bone extracts from control and LAP/Acp5-deficient animals, and analysed using antibodies to osteopontin. Note that the osteopontin immunoreactive bands have disappeared during incubation with control bone extracts while in LAP/Acp5-deficient bone extracts, the immunoreactivity is preserved. (B) Using anti-phosphoserine antibodies, the lack of dephosphorylation of osteopontin after incubation with LAP/Acp5 bone extracts is evident. The serine-phosphorylated osteopontin has disappeared after incubation with bone extracts from control mice. (C) In the presence of proteinase inhibitors, the immunoreactivity is still lost with control bone extracts, whereas inhibition of phosphatase activities with L-tartrate and molybdate prevented dephosphorylation of osteopontin.

The increased labelling density for sWGA and PNA in Kupffer cells, growth plates and calvarial bone may point to an accumulation of related substrates for both phosphatases in these tissues. However, the identities of the lectin-binding constituents are still unknown. It needs to be determined if the increased amounts of bone sialoprotein and chondrocalcin in LAP/Acp5 doubly deficient bones contribute to the increased labelling with sWGA.

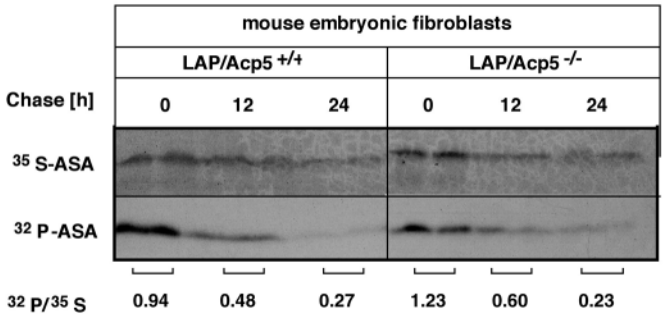


**Fig. 8.** Normal dephosphorylation of arylsulfatase A in LAP/Acp5-deficient fibroblasts. Control (*Lap*/*Acp5*$^{+/+}$) and doubly deficient (*Lap*/*Acp5*$^{-/-}$) mouse embryonic fibroblasts were labelled for 6 hours with [$^{35}$S] or [$^{32}$P]arylsulfatase A and subsequently chased with non labelled medium up to 24 hours. The disappearance of the labelled arylsulfatase A is followed and the ratio of [$^{32}$P]/[$^{35}$S]arylsulfatase A is calculated indicating normal dephosphorylation of arylsulfatase A.

## Dephosphorylation of mannose 6-phosphate residues of lysosomal enzymes

As Kupffer cells from control mice did not show dephosphorylation of endocytosed $^{32}$P-labelled arylsulfatase A (data not shown) we analysed the possible function of both phosphatases in dephosphorylation of mannose 6-phosphate residues in embryonic fibroblasts. Both control and LAP/Acp5-deficient fibroblasts dephosphorylated arylsulfatase A, showing that LAP and Acp5 are not crucial for dephosphorylation of lysosomal enzymes in cells like fibroblasts.

## Conclusions

The lysosomal phosphatases LAP and Acp5 can at least partially compensate for each other. LAP and Acp5 fulfil crucial functions in lysosomal catabolism, as exemplified by the extensive lysosomal storage in numerous cell types. It is conceivable that in some cell types, such as osteoclasts, the two lysosomal phosphatases act in sequence in a tightly controlled manner.

We thank Nicole Leister, Annegret Wais, Dagmar Niemeier, Monika Grell, Kees Hoeben, Maureen Arora, Roy Radcliffe and Wikky Tigchelaar for excellent technical assistance, Colin Gray for conducting in vitro bone formation, Maureen Arora for help with isolated osteoclastic resorption assays, and Prof. Dr G. F. J. M. Vrensen of The Netherlands Ophthalmic Research Institute, Amsterdam for his help in the EDX analyses. This work was supported by the Deutsche Forschungsgemeinschaft. A. H. was supported by the Arthritis Research Campaign. A. S. was supported by the Boehringer Ingelheim Fond.

## REFERENCES


**Andersson, G. and Ek-Rylander, B.** (1995). The tartrate-resistant purple acid phosphatase of bone osteoclasts-a protein phosphatase with multivalent substrate specificity and regulation. *Acta Orthop. Scand.* **266**, 189-194.

**Bevilacqua, M., Lord, D. K., Cross, N. C., Whitaker, K. B., Moss, D. W. and Cox T. M.** (1991). Regulation and expression of type V (tartrate-resistant) acid phosphatase in human mononuclear phagocytes. *Mol. Biol. Med.* **8**, 135-140.

**Braun, M., Waheed, A. and von Figura, K.** (1989). Lysosomal acid phosphatase is transported to lysosomes via the cell surface. *EMBO J.* **8**, 3633-3640.

**Bresciani, R., Peters, C. and von Figura, K.** (1992). Lysosomal acid phosphatase is not involved in the dephosphorylation of mannose 6-phosphate containing lysosomal proteins. *Eur. J. Cell Biol.* **58**, 57-61.

**Bresciani, R. and von Figura, K.** (1996). Dephosphorylation of the mannose-6-phosphate recognition marker is localized in later compartments of the endocytic route. Identification of purple acid phosphatase (uteroferrin) as the candidate phosphatase. *Eur. J. Biochem.* **238**, 669-674.

**Bune, A. G., Hayman, A. R., Evans, M. and Cox, T. M.** (2000). Mice lacking tartrate-resistant acid phosphatase (Acp5) have disordered macrophage inflammatory responses and reduced clearance of the pathogen *Staphylococcus aureus*. *Immunology* **102**, 103-113.

**Clark, S. A., Ambrose, W. W., Anderson, T. R., Terrell, R. S. and Toverud, S. U.** (1989). Ultrastructural localization of tartrate-resistant, purple acid phosphatase in rat osteoclasts by histochemistry and immunocytochemistry. *J. Bone Miner. Res.* **4**, 399-405.

**de Araujo, P. S., Mies, V. and Orlando, M.** (1976). Subcellular distribution of low- and high-molecular-weight acid phosphatases. *Biochem. Biophys. Acta* **452**, 121-130.

**Drexler, H. G. and Gignac, S. M.** (1994). Characterization and expression of tartrate-resistant acid phosphatase (TRAP) in hematopoietic cells. *Leukemia* **8**, 359-368.

**Echetebu, Z. O., Cox, T. M. and Moss, D. W.** (1987). Antibodies to porcine uteroferrin used in measurement of human tartrate-resistant acid phosphatase. *Clin. Chem.* **33**, 1832-1836.

**Ek-Rylander, B., Flores, M., Wendel, M., Heinegard, D. and Andersson, G.** (1994). Dephosphorylation of osteopontin and bone sialoprotein by osteoclastic tartrate-resistant acid phosphatase. Modulation of osteoclast adhesion in vitro. *J. Biol. Chem.* **269**, 14853-14856.

**Flores, M. E., Norgard, M., Heinegard, D., Reinholt, F. P. and Andersson, G.** (1992). RGD-directed attachment of isolated rat osteoclasts to osteopontin, bone sialoprotein, and fibronectin. *Exp. Cell Res.* **201**, 526-530.

**Gieselmann, V., Hasilik, A. and von Figura, K.** (1984). Tartrate-inhibitable acid phosphatase. Purification from placenta, characterization and subcellular distribution in fibroblasts. *Hoppe-Seyler's Z. Physiol. Chem.* **365**, 651-660.

**Gottschalk, S., Waheed, A., Schmidt, B., Laidler, P. and von Figura, K.** (1989). Sequential processing of lysosomal acid phosphatase by a cytoplasmic thiol proteinase and a lysosomal aspartyl proteinase. *EMBO J.* **8**, 3215-3219.

**Hayman, A. R., Jones, S. J., Boyde, A., Foster, D., Colledge, W. H., Carlton, M. B., Evans, M. J. and Cox, T. M.** (1996). Mice lacking tartrate-resistant acid phosphatase (Acp 5) have disrupted endochondral ossification and mild osteopetrosis. *Development* **122**, 3151-3162.

**Hayman, R. A., Bune, A. J., Bradley, J. R., Rashbass, J. and Cox, T. M.** (2000). Osteoclastic tartrate-resistant acid phosphatase (Acp 5): its localization to dendritic cells and diverse murine tissues. *J. Histochem. Cytochem.* **48**, 219-227.

**Hille, A., Klumperman, J., Geuze, H. J., Peters, C., Brodsky, F. M. and von Figura, K.** (1992). Lysosomal acid phosphatase is internalized via clathrin-coated pits. *Eur. J. Cell Biol.* **59**, 106-115.

**Kasper, D., Dittmer, F., von Figura, K. and Pohlmann, R.** (1996). Neither type of mannose 6-phosphate receptor is sufficient for targeting of lysosomal enzymes along intracellular routes. *J. Cell Biol.* **134**, 615-623.

**Köpf-Maier, P.** (1990). The phosphorus content of lysosomes in hepatocytes and Kupffer cells. A study using electron-spectroscopic imaging. *Acta Anat.* **139**, 164-172.

**McKee, M. D. and Nanci, A.** (1996). Osteopontin at mineralized tissue interfaces in bone, teeth, and osseointegrated implants: ultrastructural distribution and implications for mineralized tissue formation,turnover, and repair. *Microsc. Res. Tech.* **33**, 141-164.

**Minkin, C.** (1982). Bone acid phosphatase: tartrate-resistant acid phosphatase as a marker of osteoclast function. *Calcif. Tissue Int.* **34**, 285-290.

**Nyhan, W. L. and Ozand, P. T.** (1998). Lipid storage disorders. In *Atlas Metabolic Disease*. 1st edn (ed. W. L. Nyhyn and P. L. Ozand), pp. 532-614. London: Chapman & Hall.

**Pohlmann, R., Wendland, M., Boecker, C. and von Figura, K.** (1995). The two mannose 6-phosphate receptors transport distinct complements of lysosomal proteins. *J. Biol. Chem.* **270**, 27311-27318.

**Saftig, P., Hartmann, D., Lüllmann-Rauch, R., Wolff, J., Evers, M., Köster, A., Hetman, M., von Figura, K. and Peters, C.** (1997). Mice deficient in lysosomal acid phosphatase develop lysosomal storage in the kidney and central nervous system. *J. Biol. Chem.* **272**, 18628- 18634.

**Sandholzer, U., von Figura, K. and Pohlmann, R.** (2000). Function and properties of chimeric MPR 46-MPR 300 mannose 6-phosphate receptors. *J. Biol. Chem.* **275**, 14132-14138.

**Vihko, P., Virkunen, P., Hentu, P., Roiko, K., Solin, T. and Huhtala, M. L.** (1988). Molecular cloning and sequence analysis of cDNA encoding human prostatic acid phosphatase. *FEBS Lett.* **236**, 275-281.

**Vincent, J. B. and Averill B. A.** (1990). An enzyme with a double identity: purple acid phosphatase and tartrate-resistant acid phosphatase. *FASEB J.* **4**, 3009-3014.

**Waheed, A., van Etten, R. L., Gieselmann, V. and von Figura, K.** (1985). Immunological characterization of human acid phosphatase gene products. *Biochem. Genet.* **23**,309-319.

**Yaziji, H., Janckila, A. J., Lear, S. C., Martin, A. W. and Yam, L. T.** (1995). Immunohistochemical detection of tartrate-resistant acid phosphatase in non-hematopoietic human tissues. *Am. J. Clin. Pathol.* **104**, 397-402.